JOURNAL OF MATERIAL SCIENCE 11 (1976) 1817–1825

The influence of stress distribution on the deformation and fracture behaviour of ceramic materials under compression creep conditions

J.M.BIRCH, B. WILSHIRE, D.J.R. OWEN*, D. SHANTARAM*
*Department of Metallurgy and Materials Technology, and *Department of Civil Engineering, University College of Swansea, Singleton Park, Swansea, UK*

The stress distribution developed in test pieces during compression creep has been determined using the finite element method. The analyses are shown to account precisely for the inhomogeneous distribution of grain-boundary cracks developed during creep of polycrystalline magnesia and indicate that the accommodation of grain-boundary sliding by cavity formation is the rate-controlling process during high temperature creep of reaction-bonded silicon nitride.

1. Introduction

The experimental difficulties associated with the study of the creep behaviour of ceramic materials in tension [1] has led to the extensive use of bend or compression testing procedures. The bend test, although comparatively simple to perform, involves assumptions about the material behaviour in the simple solutions for stress and strain which appear to be invalid under creep conditions [2, 3]. Furthermore, since the stress and strain-rate varies throughout the specimen during a bend test, interpretation of results is difficult. Even with compression testing, which appears to give a simple uni-axial stress system, several experimental difficulties can be encountered.

With cylindrical compression specimens, if the ratio of the height (h) to diameter (d) is large, buckling can occur, whereas a low ratio can result in barrelling of the specimen because of specimen end constraint [4]. A compromise between these two effects has been reported [5] to exist with h/d ratios in the range 1.5 to 2.5.

Although compression creep tests are normally carried out using cylindrical specimens, this type of specimen can introduce difficulties of alignment when small diameter specimens are used to minimize the applied load needed with high strength materials. Since the specimen extension is normally measured with extensometer rods attached to platens in contact with the specimens, incorrect strain measurements may also result with high strength samples because of identation of the platens. These problems can be overcome by using a dumb-bell shaped specimen (Fig. 1). In this case, the enlarged sample ends prevent indentation of the platens and facilitates specimen handling and alignment. At room temperature, little difference has been found between strength measurements determined using dumb-bell and

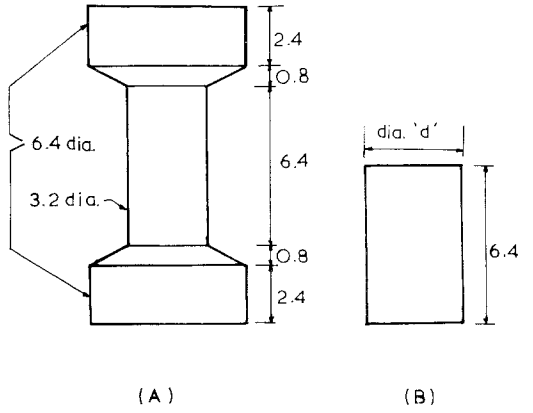

Figure 1 Dimensions (mm) of (A) dumb-bell and (B) cylindrical specimens. Dimension $d = 4.25$ for MgO and $d = 3.18$ for reaction-bonded silicon nitride specimens.

cylindrical specimens [1] but no comparison appears to have been made under creep conditions.

A further difficulty with compression creep testing has been illustrated in a recent study [6] of the development of grain-boundary cavities and cracks during creep of polycrystalline magnesia. The cavities and cracks formed predominantly on boundaries parallel to the compression axis, indicating that tensile stresses are developed across these boundaries. However, cracks did not develop uniformly throughout the cylindrical specimens used, with "dead-zones" extending from the specimen ends in which no crack formation could be detected (Fig. 2). This suggests that the stress distribution established during compression creep testing is not uniform under practical conditions of specimen end restraint.

In the present work, the stress distribution in compression has been analysed using the finite element method, a powerful technique which is being increasingly applied to problems of ceramic component design [7, 8]. As well as investigating the behaviour of dumb-bell and cylindrically shaped specimens, the results of the stress analysis have been compared with the compression creep and fracture characteristics of reaction-bonded silicon nitride, a material in which gross plasticity is not observed [9], and polycrystalline magnesia; a material which exhibits comparatively large strains in compression [6].

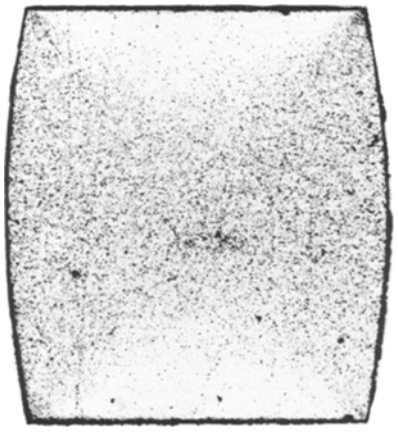

Figure 2 Longitudinal section of MgO specimen after 16% creep strain at 96 MN m^{-2} and 1596 K, × 10.

2. Experimental procedure

The magnesia was supplied in the form of sintered bars (6.4 mm × 6.4 mm × 32.0 mm) by the Steetley Co Ltd. Specially prepared $Mg(OH)_2$ was calcined at 1573 K, pressed into bars and sintered at 1923 K to produce material of 93 to 95% theoretical density, 99.5% purity and 10 to 14 μm average grain diameter. Cylindrical test-pieces (4.25 mm diameter and 6.4 mm long) were prepared from the bars, a polishing jig being used to ensure that the specimen ends were flat and parallel.

The reaction-bonded silicon nitride (RBSN) was supplied by the Admiralty Materials Laboratory. The structure and properties of RBSN has been widely reported [10, 11]. For the present work, silicon powder was compacted into bars, then machined to give dumb-bell shaped specimens (Fig. 1) which were subsequently nitrided. The present batch of samples had an average weight gain of 64% during nitriding, a density of ~2.6 Mg m^{-3} and a room temperature bend strength of 248 MN m^{-2}. Cylindrical specimens of RBSN (Fig. 1) were produced from the dumb-bells by polishing away the enlarged ends.

Compression tests were performed using a high precision, constant stress machine which has been described previously [12]. Using this equipment, it has been established that, when cylindrical test pieces of the polycrystalline magnesia were compressed between reaction-bonded silicon nitride platens, no detectable impression was made on the platens even after many successive creep tests. In the present work, silicon nitride platens were also found to be perfectly adequate for the tests with the RBSN dumb-bells but silicon carbide was used to avoid indentation with the RBSN cylinders.

3. Stress analysis

The method of solution employed was the finite element technique which is a generalization of the stiffness method of structural analysis. Its basis lies in the subdivision of the structure into a discrete number of finite sized elements in each of which an assumed variation of the unknown quantities (usually displacements) is postulated. Continuity of the unknown across inter-element boundaries is invoked at only a finite number of points termed nodal points.

The method has the great advantage of being able to accommodate discontinuities and irregular-

ities in material properties and geometry with ease and at present is probably the only feasible general method of solution of structures composed of materials with non-linear deformation characteristics. The finite element method is adequately explained in [13] and the details of its extension to the realm of non-linear material behaviour are to be found in [14].

Recent advances in both equation solution algorithms and individual element characteristics have resulted in the development of an economical computer program for the solution of elasto-plastic problems [14]. Either small or large displacement problems can be accommodated subject to the restriction of small strains. The program, employing the isoparametric element concept, can readily incorporate any yield criterion for isotropic materials obeying the normality rule of plasticity with isotropic and or kinematic hardening properties. A general purpose solution algorithm is included from which three options are available depending on the type of problem to be solved. Each method is based on the satisfaction of equilibrium by the re-distribution of residual forces.

For the present study, the Von Mises yield criterion was adopted, the input information required being the elastic modulus, E, Poisson's ratio, ν, and the uniaxial yield stress, σ_y, of the material. The material behaviour after initial yield is determined by the effective stress versus effective plastic strain characteristic which, for the purpose of the numerical analysis, is prescribed in a piecewise linear manner.

The output quantities are displacements, stresses and strain at each nodal point as well as stresses and strains at several selected points (Gaussian integration points) within each element.

The inhomogeneous stress distribution in compression specimens is a consequence of the frictional restraint on lateral spreading of the specimen ends [4]. The present analysis was carried out using completely restrained ends and is thus an upper bound solution. However, in view of the difficulties of lubricating the platen–specimen interface when testing ceramics at high temperatures, it is likely to be a close approximation to the actual conditions. Certainly the barelling observed at high strains is very marked [6]. In the case of RBSN which does not yield [9] at the mean applied compressive stress of 345 $MN\,m^{-2}$, the elastic solution is used to obtain the stress distribution (Fig. 3). The material constants necessary for the calculation were taken as Young's modulus $18 \times 10^4 MN\,m^{-2}$ [15] and Poisson's ratio = 0.24 [8].

For the MgO, which yields at $\sim 50\,MN\,m^{-2}$ [16] the elastic-plastic solution holds with Young's modulus = $20 \times 10^4 MN\,m^{-2}$ [17] and Poisson's ratio = 0.33 [18]. The coefficient of strain hardening which holds between the yield stress and the applied load of $96\,MN\,m^{-2}$ was taken to be $5 \times 10^3\,MN\,m^{-2}$ [19]. The stress distribution is shown in Fig. 4.

4. Experimental results

4.1. Transient and steady-state creep curves

For creep tests carried out at 1600 K with the polycrystalline magnesia, it has been demonstrated [18] that the high initial creep rates, observed immediately following the instantaneous specimen strain on loading decreased continuously until a constant or steady-state creep rate was attained. At creep strains above ~7%, the creep rate then accelerated gradually as detectable barelling of the specimen occurred. The steady creep rate recorded under the same test conditions for different specimens varied by only ±15% [12]. Furthermore, no significant change in creep rate was noted by varying the height-to-diameter ratio of the cylindrical testpieces over the range 1.1 to 2.0.

The form of the creep curves obtained for the RBSN (Fig. 5) at temperatures within the range 1550 to 1650 K was found to be similar to that for the magnesia, although the creep strains observed were comparatively low. Results obtained for a number of different specimens showed that the steady creep rate was reproducible to ±20%, a value comparable with that reported for commercial creep resistant alloys [20]. Comparison of the creep curves recorded with cylindrical and dumb-bell shaped testpieces (Fig. 5) showed that, although the initial creep rates and the transient creep strains were slightly greater with the dumb-bell specimens, the creep rates eventually attained were similar. Over the temperature range studied, the creep behaviour of RBSN was found to be not markedly affected by oxidation of the specimens. Creep tests carried out in argon atmosphere indicated that the creep rates attained were only ~20% slower than those obtained in air. Furthermore, samples which were preheat-treated for 360 ksec in air at 1623 K prior to creep testing,

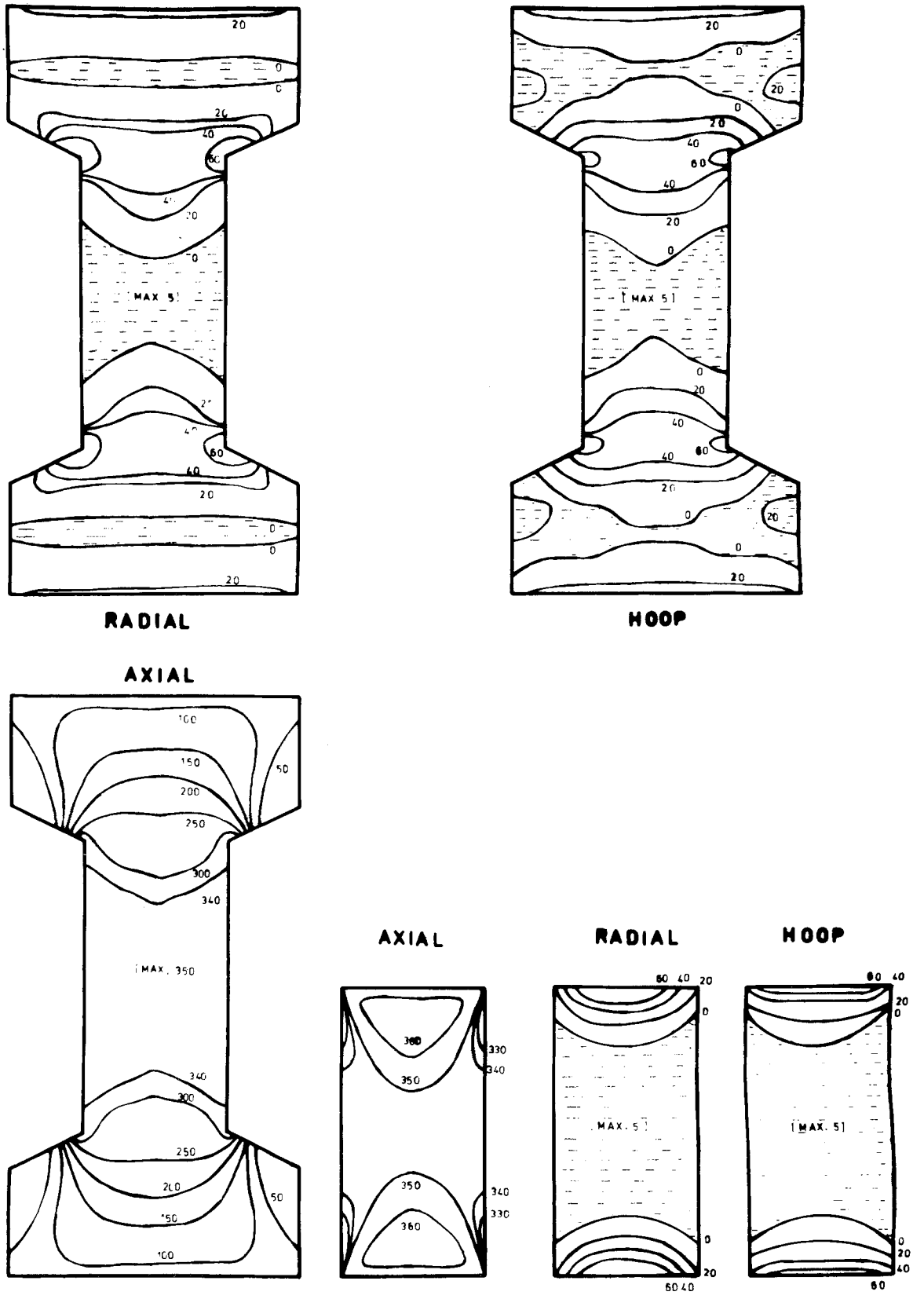

Figure 3 Distribution of axial, radial and hoop stress ($MN\,m^{-2}$) in dumb-bell and cylindrical specimens of reaction-bonded silicon nitride under a nominal axial compressive stress of 345 $MN\,m^{-2}$. Shading denotes tension.

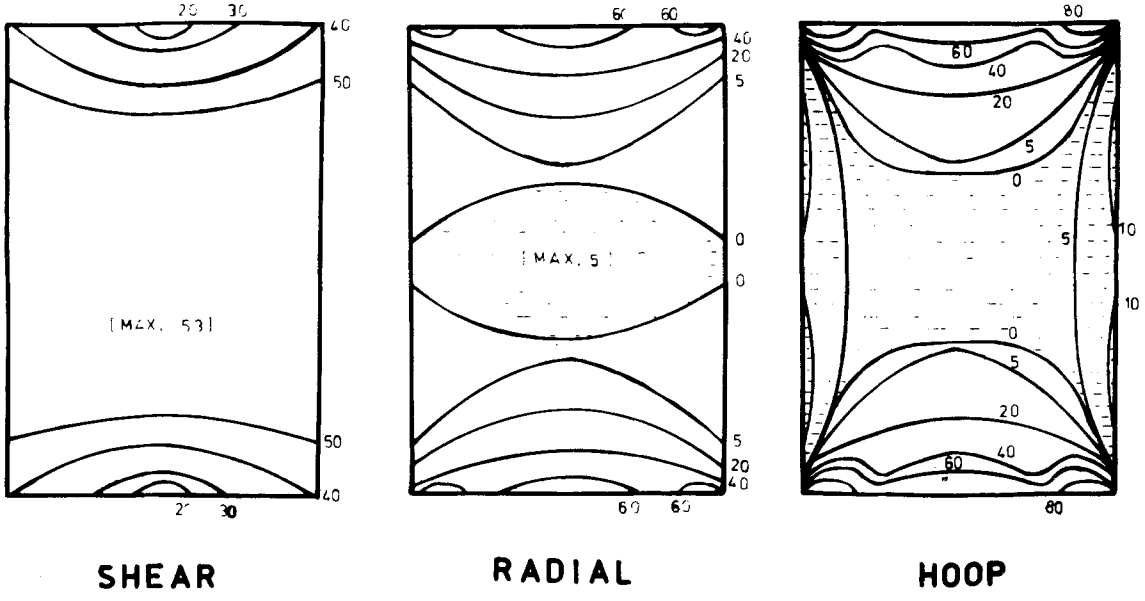

Figure 4 Distribution of shear, radial and hoop stress ($MN\,m^{-2}$) in specimens of MgO under a nomial axial compressive stress of 96 $MN\,m^{-2}$.

at 1623 K, exhibited identical behaviour to that of unheat-treated specimens.

4.2. Stress and temperature dependence of creep

An indication of the processes controlling the rate of creep deformation may be obtained [21] by determining the dependence of the steady-state creep rate ϵ_S, on stress, σ, grain diameter, d, and temperature, T, as

$$\dot{\epsilon}_S = A\left(\frac{1}{d}\right)^m \sigma^n \exp -\frac{Q_c}{RT}$$

where A, m and n are constant, R is the gas constant and Q_c is the activation energy for creep. Each creep mechanism then predicts a definite value for m, n and Q_c.

For the polycrystalline magnesia, $n = 3$ [12] in agreement with other workers [22, 23], the creep rate is independent ($m = 0$) of grain size [22] and $Q_c = 450\,kJ\,mol^{-1}$ [24] comparable with the activation energy for oxygen ion diffusion in MgO [25].

With the RBSN, to eliminate any possible error as a result of specimen-to-specimen variations, the stress exponent, n, was determined both by

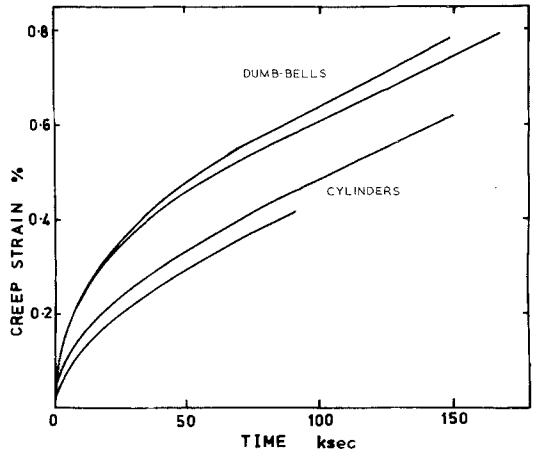

Figure 5 Creep curves recorded at 1623 K and 345 MN m^{-2} for dumb-bell and cylindrical specimens of reaction-bonded silicon nitride.

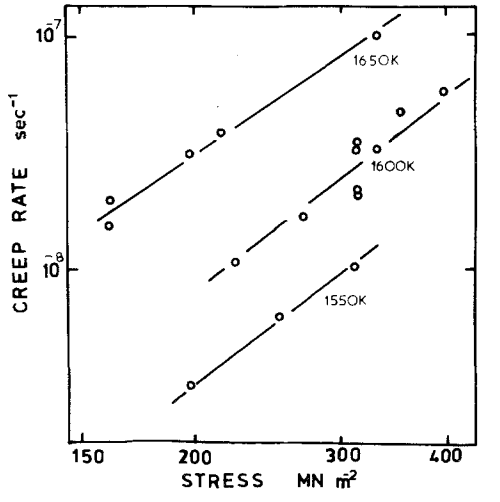

Figure 6 Stress dependence of the steady creep rate of reaction-bonded silicon nitride.

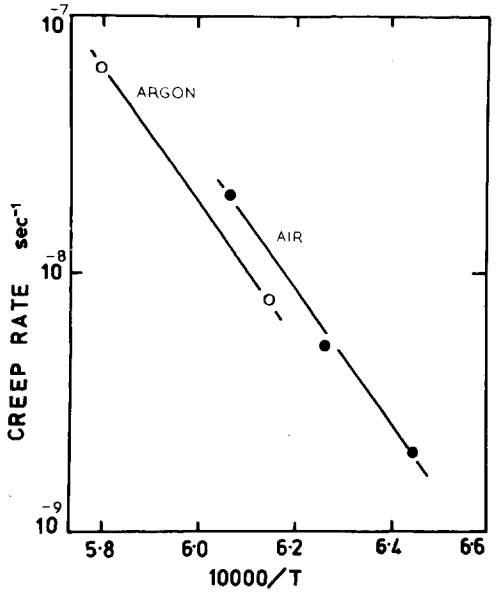

Figure 7 Temperature dependence of the steady creep rate of reaction-bonded silicon nitride tested in air and argon at 165 MN m^{-2}.

measuring the creep rates obtained on different specimens over a range of stresses and also by monitoring the changes in steady creep rate following stress increases with the same sample. With both methods, $n = 2.3$ (Fig. 6). Similarly, the activation energy for creep was obtained from the variation in steady creep rate for different samples tested at the same stress over a range of temperatures and also from the change in steady creep rate following a small temperature change during individual tests. Again, with both methods, $Q_c = 650\,\text{kJ mol}^{-1}$ (Fig. 7), illustrating the excellent reproducibility of the results obtained with this material. With the multiphase RBSN, the crystal size is both non-uniform and extremely fine so that no attempt to establish a grian-size dependence was made.

4.3. The development of grain-boundary cracks during compressive creep

Microstructural examination of longitudinal sections of testpieces of polycrystalline magnesia after various creep strains has demonstrated that cavities and cracks develop predominantly on grain boundaries parallel to the compression axis, illustrating that tensile stresses are developed across boundaries of this orientation [6]. In the present investigation, a detailed study has been made of the incidence of cracking by examination of transverse sections of polycrystalline magnesia crept to 7% strain.

Transverse sections were taken at the mid-height position of the specimens and the crack incidence determined for two regions, one near the centre of the specimen (i.e. within a radius of 500 μm from the centre) and the other near the specimen edge (i.e. in the region from ~200 to 500 μm of the edge). For each region, about 20 areas (each containing about 20 boundaries) were inspected. In all cases, boundaries were examined to determine their angle with respect to the radius of the specimen on the polished section and whether or not cavities or cracks had developed on them. For each region, the boundaries were then grouped into three angle intervals, 0 to 30°, 30 to 60° and 60 to 90° to the specimen radius. The number of boundaries on which cracks had formed was calculated, for each angle interval, as a percentage of the total number of cracked boundaries in the areas examined (Table I). Clearly, the incidence of cracking for boundaries nearly perpendicular to the radius is greater near the centre than the edge of the specimen, whereas the incidence for boundaries approximately parallel to the radius is greater near the specimen edge. For both regions, the incidence of cracking on boundaries at ~45° to the radius is comparatively low.

It was not possible to conduct a similar survey for the RBSN since the material has a high porosity (~15%) and such a fine structure that cavity or crack development between grains was difficult to observe. Furthermore, density measurements, which are sufficiently sensitive to detect the very small changes associated with crack formation [6] are rendered difficult by the open porosity and the surface oxidation occurring during creep.

5. Discussion

5.1. The influence of specimen geometry on creep behaviour

RBSN does not exhibit gross plasticity in compression under the present conditions of stress and temperature [9]. Thus, the stress distribution following loading to the creep stress for the cylindrical and dumb-bell shaped specimens of RBSN should be given by the elastic solution (Fig. 3a and b). With both specimen types, the stress distribution along the gauge length is similar. Regions exist where the radial and hoop stresses are tensile

in nature, although the values are low compared with the applied compressive stress.

The initial creep rates and the transient creep strains are slightly larger for the dumb-bells than for the cylindrical testpieces (Fig. 5). This may be a consequence of some deformation occurring in the ends of the dumb-bells resulting, in effect, in a longer deforming length with the dumb-bell specimens. However, the steady creep rate eventually attained (Fig. 5) and the stress distribution developed within the gauge lengths (Fig. 3a and b) are similar for both types of specimen. Thus, with high strength materials which do not exhibit large creep strains, dumb-bell shaped specimens can be used when this type of specimen offers practical advantages.

5.2. The distribution of grain-boundary cavities and cracks during compression creep

During high temperature creep, grain-boundary cavities and cracks form preferentially on boundaries across which exists the maximum tensile stress. With the polycrystalline magnesia, "dead-zones" were observed extending from the specimen ends in which no crack formation could be detected during compression creep (Fig. 2). In the "dead-zones", the stresses across the grain boundaries are invariably compressive in nature (Fig. 4) so that crack formation would not be expected.

Examination of polished longitudinal sections of magnesia [6] has shown that, away from the "dead-zones", cracks occur predominantly on boundaries parallel to the compression axis. The stress analysis illustrates that tensile radial and hoop stresses develop across these boundaries (Fig. 4). Furthermore, the examination of the crack distribution on the transverse sections (Table I) demonstrates that the incidence of cracking for boundaries nearly perpendicular to the radius is greater near the centre than the edge of the specimen, whereas the incidence for boundaries approximately parallel to the radius is greater near the specimen edge. This distribution is directly in agreement with the calculated stress distribution in that the tensile radial stresses are highest at the specimen centre whilst the tensile hoop stresses are greatest towards the specimen edge.

TABLE I Crack distribution for transverse sections of polycrystalline MgO crept to a strain of 7% at 1596 K and 96 MN m^{-2}

	Boundary angle relative to radii		
	0–30°	30–60°	60–90°
No. of cracks as % of total	edge 60 ± 3	19 ± 2	21 ± 1
	centre 49 ± 2	19 ± 1	32 ± 1

5.3. Stress distribution in relation to deformation processes during creep

With magnesia, determination of the dependence of the steady creep rate on stress and temperature (Equation 1), combined with studies of the dislocation structures developed during creep, have demonstrated that creep is a result of the generation and movement of dislocations. In particular, studies of the strain/time behaviour following small stress changes during creep suggest that the rate-controlling process during creep of magnesia is the growth of the three-dimensional dislocation network present within subgrains, to form dislocation sources allowing slip to occur. The activation energy for creep ($Q_c = 460$ kJ mol^{-1}) then reflects the diffusion controlled growth of the network dependent on oxygen ion transport through the MgO lattice [25], whilst the stress exponent, n ($\simeq 3$) is compatible with the stress dependence of the rate of network growth [26].

With RBSN, the observed dependence (Figs. 6 and 7) of the steady creep rate on stress ($n = 2.3$) and temperature ($Q_c = 650$ kJ mol^{-1}) are similar to those reported for RBSN in bend [27] and for HPSN in bend and tension [28, 29]. This suggests that the mechanism of creep is essentially the same for both hot pressed and reaction-bonded silicon nitride. Although dislocations have been detected in HPSN [30], it is generally considered that plastic strain within the grains can play only a minor role in the deformation of silicon nitride. Instead, grain-boundary sliding is considered to be the main deformation mode during creep. This interpretation is supported by the observation that the addition of ceria to HPSN, which increases the refractoriness of the grain-boundary phase, reduces the creep rate and increases the activation energy for creep [31]. An alternative suggestion is that the rate-controlling process during creep of silicon nitride is not sliding but the accommodation of sliding by grain-boundary cavity development [32]. A creep model [33] based on the deformation rate being controlled by cavity and crack formation can account for the

stress exponent ($n \simeq 2$) observed for both hot-pressed and reaction-bonded silicon nitride.

The present work appears to offer a method of distinguishing between sliding and cavity development as the rate-controlling process during creep of silicon nitride. A major feature of the results reported for HPSN is the observation that, in order to obtain the same creep rate, the applied stress needed in a compression test is about an order of magnitude greater than is required in tension [28]. If grain-boundary sliding is the rate-controlling process, then the rate of sliding would be expected to be determined by the shear stresses acting along the boundaries. On this basis, under the same applied stress in tension and compression, the shear stresses developed would be similar so that the rate of sliding, and hence the creep rate, should be essentially the same contrary to the experimental observations [28]. However, the present work shows that, in a compression test, the maximum tensile stresses developed are only about a tenth of the applied compressive stress. Since the results obtained with magnesia demonstrate that the formation of cavities and cracks depends on the tensile stresses developed across boundaries, the tenfold difference required to obtain the same creep rate in tension and compression can be accounted for if the cavity formation necessary to accommodate sliding, rather than the sliding itself, is the rate-controlling process during creep of silicon nitride.

6. Conclusions

The results of a finite element analysis of the stress distribution developed in test pieces during compression creep, considered in relation to an experimental study of the creep and fracture behaviour of polycrystalline magnesia and reaction-bonded silicon nitride, suggest that:

(1) the creep and fracture behaviour exhibited by cylindrical and dumb-bell shaped testpieces are essentially the same under compression creep conditions;

(2) grain-boundary cavities and cracks form only in regions of the testpiece where tensile stresses are developed across the grain boundaries;

(3) the rate-controlling process during creep of silicon nitride is the accommodation of grain-boundary sliding by cavity formation.

Acknowledgements

The authors wish to thank the Procurement Executive, Ministry of Defence for supporting this work. The encouragement given by Dr. D.J. Godfrey of the Admiralty Materials Laboratory is greatefully acknowledged.

References

1. S. A. BORTZ and T. A. WADE, "Structural Ceramics and Testing of Brittle Materials", edited by S.J. Acquaviva and S.A. Bortz (Gordon and Breach New York, 1967).
2. C. A. ANDERSON, D. P. WEI and R. KOSSOWSKY, "Deformation of Ceramics, edited by R.C. Brant and R. Tressler (Plenum, New York, 1975)
3. C. A. ANDERSON, Scientific Paper 75-9D4-FORAM P2, Westinghouse Corp, Pittsburg (1975).
4. D. R. CROPPER and J. A. PASK, *Amer. Ceram. Soc. Bull* **48** (1969) 555.
5. A. CROSBY and P. E. EVANS, *J. Mater. Sci.* **8** (1973) 1573.
6. J. M. BIRCH, P. J. KING and B. WILSHIRE, *ibid* **10** (1975) 175.
7. J. A. JEYES, D. J. LINES and S. M. MANTON, *Proc. Brit. Ceram. Soc.* **22** (1973) 397.
8. R. N. KATZ and A. F. McLEAN, *ibid* **22** (1973) 409.
9. A. G. EVANS and R. W. DAVIDGE, *J. Mater. Sci.* **6** (1971) 1292.
10. B. J. DALGLEISH and P. L. PRATT, *Proc. Brit. Ceram. Soc.* **22** (1973) 323.
11. D. J. GODFREY and M. W. LINDLEY, *ibid* **22** (1973) 229.
12. J. M. BIRCH and B. WILSHIRE, *J. Mater. Sci.* **9** (1974) 794.
13. O. C. ZIENKIEWICZ, "The Finite Element Method in Engineering Science" (McGraw-Hill, New York, 1971).
14. D. R. J. OWEN, G. C. NAYAK, A. P. KFOURI and J. R. GRIFFITHS, *Int. J. Num. Methods* **6** (1973) 63.
15. J. T. BARNBY and R. A. TAYLOR, "Special Ceramics 5" (Brit. Ceram. Res. Assoc., Stoke-on-Trent, 1970) p.311.
16. A. G. EVANS, D. GILLING and R. W. DAVIDGE, *J. Mater. Sci.* **5** (1970) 187.
17. J. B. WACHTMAN and D. G. LAM, *J. Amer. Ceram. Soc.* **42** (1959) 254.
18. G. V. SAMSONOV, "The Oxide Handbook" (Plenum, New York, p. 233.
19. J. M. BIRCH and B. WILSHIRE, *J. Mater. Sci.* **9** (1974) 871.
20. P. W. DAVIES, J. P. DENNISON and D. SIDEY, *J. Inst. Met.* **101** (1973) 153.
21. T. G. LANGDON, D. R. CROPPER and J. A. PASK, "Ceramics in Severe Environment", edited by W.W. Kriegel and H. Palmour (Plenum, New York, 1971) p. 297.

22. T. G. LANGDON and J. A. PASK, *Acta Met.* **18** (1970) 505.
23. J. B. BILDE-SORENSON, *J. Amer. Ceram. Soc.* **55** (1972) 600.
24. J. M. BIRCH and B. WILSHIRE, *Proc. Brit. Ceram. Soc.* **25** (1975) 127.
25. J. NARAYAN and J. WASHBURN, *Acta. Met.* **21** (1973) 523.
26. J. FRIEDEL, "Dislocations" (Pergamon Press, London, 1964)
27. W. ENGEL and F. THUMMLER, *Ber. Dt. Keram. Ges.* **50** (1973) 204.
28. R. KOSSOWSKY, D. G. MILLAR and E. S. DIAZ, *J. Mater. Sci.* **10** (1975) 913.
29. S. DIN and P. S. NICHOLSON, *ibid* **10** (1975) 1375.
30. A. G. EVANS and J. V. SHARP, *ibid* **6** (1971) 1292.
31. K. S. MAZDIAYASNI and C. M. COOKE, *J. Amer. Ceram. Soc.* **57** (1974) 536.
32. F. F. LANGE, "Deformation of Ceramics", edited by R.C. Brant and R. Tressler (Plenum, New York, 1975).
33. A. CROSBY and P. E. EVANS, *J. Mater. Sci.* 8 (1973) 1579.

Received 9 March and accepted 2 April 1976.